Amplified spontaneous emission over the XeF($D \rightarrow X$) transition in solid Kr

H. Kunttu, W. G. Lawrence, and V. A. Apkarian[a)]
Department of Chemistry, Institute for Surface and Interface Science, University of California, Irvine, California 92717

(Received 20 July 1990; accepted 17 October 1990)

XeF doped solid Kr represents a novel solid state exciplex laser. A net gain in excess of 100 cm^{-1} and a superradiant beam of 5 mrad divergence are observed over the XeF($D \rightarrow X$) transition at 301 nm, when free standing crystals of XeF doped Kr are optically pumped near the XeF($D \leftarrow X$) absorption maximum at 260 nm. Superlinear dependence of gain on pump intensity and low divergence of the amplified beam are taken as evidence for self-focusing. The XeF(D) state is effectively isolated from the lower manifold of charge transfer states in solid Kr, which includes XeF(B,C) and $(KrXe)^+F^-$.

I. INTRODUCTION

Solid state rare gas halide exciplexes represent a novel family of lasers. High energy density, high efficiency, broad tunability, low pump thresholds are among the attributes of solid state rare gas halide exciplexes. The first example of such a laser was demonstrated in a free standing crystal of argon doped with XeF, in which laser action over both XeF($B \rightarrow X$) and XeF($C \rightarrow A$) transitions were reported.[1] Gain measurements over XeF($D \rightarrow X$) in similar crystals were reported soon afterwards.[2] Given the very large gain of these systems, spectral narrowing due to amplified spontaneous emission (ASE) is observed and used to characterize the gain in the medium.[2] Contrary to early predictions of generality of principles to all solid state rare gas halides, attempts at observing gain in several systems have failed.[3] Failure to observe gain in KrF doped solid Ar has been reported.[4] The KrF charge transfer states in solid Ar relax rapidly to the mixed triatomic $(ArKr)^+F^-$ configuration and emission is exclusively observed from that state. Reabsorption by the triatomic charge transfer state is thought to preclude the possibility of gain.[3] This is consistent with our failure to observe stimulated emission in other condensed phase triatomic exciplexes, be it in solid, liquid, or supercritical phases. Among the systems studied in our laboratory are Ar_2F,[5] Kr_2F,[4] and Xe_2Cl (Ref. 6) in free standing crystals of Ar, Kr, and Xe, respectively; Xe_2Cl and Xe_2Br in liquid Xe;[7] and Xe_2Cl in supercritical fluid Xe.[8] In all of these systems, a strong reabsorption by the $Rg_2X(4\,^2\Gamma)$ state is believed to prevent net gain. Thus, the earlier reports on stimulated emission in thin films of Xe_2Cl (Ref. 9) and liquid phase Xe_2Cl (Ref. 10). are now subject to doubt. It should, however, be noted that both Kr_2F (Ref. 11) and Xe_2Cl (Ref. 12) have been made to lase by electron-beam pumping in the gas phase, despite the fact that in gas phase Kr_2F the exciplex emission is strongly reabsorbed.[13]

Solid Kr doped with atomic F and Xe represents an interesting system, since in such solids diatomic XeF and mixed triatomic XeKrF charge transfer states coexist. The details of spectroscopy and photodynamics of this system will be reported elsewhere.[14] It is observed that the XeF(C) state is strongly coupled to the triatomic, and these states are efficiently populated by energy transfer from the high-lying vibrational levels of XeF(B). In contrast, the XeF(D) state is isolated effectively from the rest of the system and $v = 0$ of XeF(D) is observed to decay radiatively. It was therefore to be expected that the $D \rightarrow X$ transition in solid Kr would also be a useful laser candidate. The verification of this expectation, despite the presence of the lower-lying charge transfer states in the system, is related in this article.

II. EXPERIMENT

XeF doped solid Kr is prepared by *in situ* photolysis of molecular fluorine in free standing crystals of F_2:Xe:Kr. The crystals are grown by condensing the premixed gas on the cold tip of a closed-cycle cryostat, through a glass mold (a glass tube of 1 cm $\times$ 1 cm square cross section). The crystal is grown at a backing pressure of 250 Torr. While the cryotip is maintained at $\sim$10 K, the temperature of the crystal during its growth rises to 35 K, as measured by a thermocouple embedded in the solid. The mold is subsequently retracted to leave behind an optically clear crystal anchored to the cryotip. This technique has been extensively developed by Schwentner and co-workers, who have characterized the solids as polycrystals with grain sizes determined by the growth conditions.[15]

Ultraviolet irradiation of F_2 doped crystalline krypton leads to efficient photodissociation of the molecules. Energy and temperature dependence of photodissociation quantum yields, which reach unity at excess energies above 2 eV, have already been reported.[16] The resulting F atoms readily diffuse at temperatures above 17 K in Kr.[5,14] Upon encountering Xe, the mobile F atoms permanently trap in the XeF(X) potential. Thus, when the photodissociation is carried out at temperatures above 20 K, the F atoms are scavenged by the Xe trap sites. Therefore, XeF number densities as high as 10^{19} cm^{-3} are in principle attainable in the present solids. This maximal number density is, however, not reached due to two main reasons: (a) due to formation of covalent xenon halides, in particular, XeF_2; (b) due to both radiative and nonradiative dissociation of the exciplexes with concomitant production of mobile F atoms.[4] Irradiation of XeF_2 in its first absorption band is known to produce XeF(X) + F efficiently.[17] Moreover, it has recently been shown that 260 nm irradiation of XeF_2 leads to efficient photodissociation in solid Ar even under high pressure (12 kbar).[18] Therefore,

[a)] Alfred P. Sloan Fellow.

 0021-9606/91/031692-06$03.00 © 1991 American Institute of Physics

Downloaded 17 Feb 2004 to 128.200.47.19. Redistribution subject to AIP license or copyright, see http://jcp.aip.org/jcp/copyright.jsp

ultraviolet irradiation of F_2/Xe/Kr samples lead to a photochemical steady state involving at least XeF_2, XeF, F_2, and F atoms trapped in the bulk of Kr, the detailed balance of which is sensitive to excitation wavelength, temperature, and initial concentrations of dopants. The complete characterization of this steady state is not yet available and as such the exact XeF number densities in the solid are not known. Both thermal diffusion and photomobility of F atoms in these doubly doped solids can be tracked conveniently by monitoring the growth in XeF emission, and the concomitant decay in Kr_2F emission, which has been reported previously.[4,5,14] The present experiments are conducted at temperatures between 20 and 35 K, and 260 nm is used as the photodissociation wavelength.

The experimental setup is shown in Fig. 1. The frequency-doubled output of an excimer-pumped dye laser (Lambda Physik MSC101/FL 2003) with a typical output energy of ~ 1 mJ at 260 nm, and a pulsewidth of 7 ns [full width at half-maximum (FWHM)], was used. The same source is used for both dissociation of F_2 and subsequent gain measurements. The pump beam is focused in the crystal, with an $f/16$ lens of 60 cm focal length. The beam shape of the doubled dye laser is ill defined. At the focal waist, an elliptic spot of $100\,\mu m \times 200\,\mu m$ is obtained. The lens is typically placed 40 cm from the crystal, yielding a spot size of $\sim 600\,\mu m$ in the crystal. Thus, under the hardest pumping conditions, the fluence at the crystal reaches ~ 100 MW cm^{-2}. Damage of the crystals becomes apparent above these power densities. The pump intensity is controlled through a variable attenuator (Newport Corp. 935-5).

The experimental arrangement allowed for monitoring of either side-light (emission at 90° to the excitation beam), or on-axis emission from the crystal. Emission spectra were recorded with an intensified diode array (EG&G OMA III) after dispersion of the emission with a 1/4 m polychromator. Excitation spectra were recorded using the monochromatized output of a 150 W Xe arc lamp, which was modulated at 1 kHz using a mechanical chopper. The dispersed emission from the crystal was recorded using a photomultiplier and lock-in amplifier. A pair of 1/3 m monochromators (McPherson 218) were used in the excitation and detection arms.

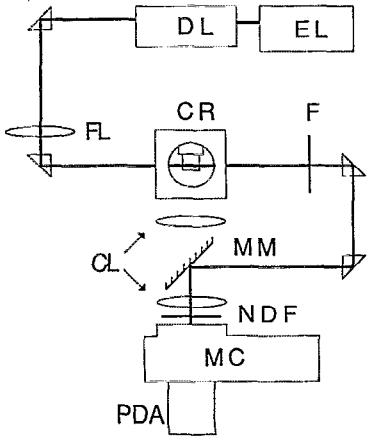

FIG. 1. Experimental setup: EL = excimer laser; DL = dye laser and BBO doubling crystal; FL = pump focusing lens; CR = cryostat with sample; F = 295 nm long-pass filter; CI = fluorescence collection optics; MM = movable mirror for line narrowing observations; NDF = neutral density filter; MC = 1/4 m monochromator; PDA = photodiode array detector.

III. RESULTS AND DISCUSSION

All of the data to be reported here pertain to solids of original F_2:Xe:Kr concentration of 1:1:3000. Upon irradiation of the transparent solid at 260 nm, a bright blue emission due to Kr_2F develops. Upon warmup of the solid above 20 K, with continuous irradiation, the emission appears whitish. An emission spectrum obtained after extensive irradiation of such a solid is shown in Fig. 2(a). The XeF $D \rightarrow X$, $D \rightarrow A$, and $B \rightarrow X$ emissions can be seen at 303, 364, and 428 nm, respectively. The XeF $C \rightarrow A$ emission, which peaks near 575 nm, is barely visible under these conditions.[3,14] Except for a red shift, these emissions follow closely those observed in solid Ar[2,3] and can be well rationalized by the gas phase diatomic potentials of XeF.[17,19,20] In addition to the diatomic emissions, a band at 465 nm can be observed, which can be assigned to the mixed triatomic XeKrF.[14] The main emission in the spectrum of Fig. 2(a) is due to fluorescence from the D state. We note that the optical multichannel analyzer used in recording this spectrum was not intensity calibrated, and that based on the manufacturer specifications, we estimate that as much as 50% of the emission is due to the lower charge transfer states. The lower manifold of charge transfer states is populated from the vibrationally excited levels in XeF(D).[14]

An excitation spectrum obtained by monitoring the $D \rightarrow X$ emission is shown in Fig. 2(b). In contrast to XeF in

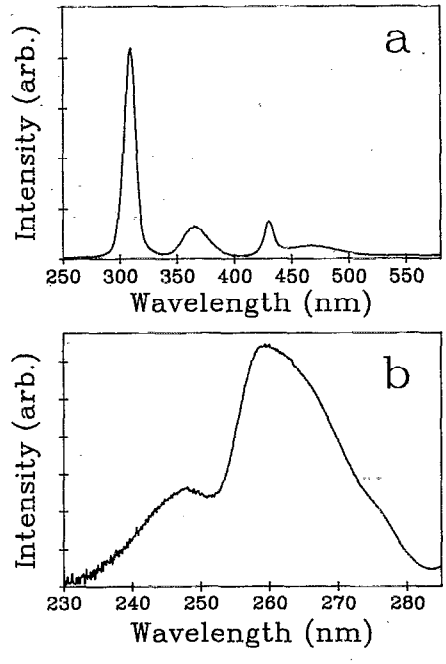

FIG. 2. (a) Emission spectrum from a F_2:Xe:Kr = 1:1:3000 crystal at 260 nm excitation. Prior to recording the spectrum, the crystal was irradiated extensively with 260 nm laser. The spectrum shows no traces of $Kr_2{}^+F^-$ emission due to several annealing cycles between 10 and 25 K. The emission bands seen are XeF($D \rightarrow A$) at 303 nm; XeF($B \rightarrow X$) at 428 nm; $(KrXe)^+F^-$ at 465 nm. The spectrum was recorded at 15 K. (b) Excitation spectrum of the XeF $D \rightarrow X$ emission at 303 nm. Original sample composition is F_2:Xe:Kr = 1:1:3000. The spectrum was recorded after overnight irradiation of the crystal with a broadband Xe arc lamp (150 W) and was recorded with monochromator slits corresponding to a 2 nm bandpass. The increase of the signal in the red end of the spectrum corresponds to the threshold of the 295 nm long-pass filter used in the experiment.

Downloaded 17 Feb 2004 to 128.200.47.19. Redistribution subject to AIP license or copyright, see http://jcp.aip.org/jcp/copyright.jsp

Ar and Ne,[21,22] the excitation spectrum in Kr does not reveal any vibrational structure. Evidently, the larger polarizability of Kr leads to a strong coupling of the exciplex to the lattice. This leads to rapid vibrational relaxation within the electronic manifold, such that the observed emission can be attributed exclusively to $v = 0$. The dip near 250 nm in the excitation spectrum is ascribed to a crossing between XeF(D) and KrXeF potentials, based on the observation that it leads to an enhancement of emission from KrXeF and XeF(C), but not XeF(B).[14]

Despite the fact that the $D \rightarrow X$ transition terminates in the bound part of the XeF(X) potential, the fluorescence of 8.2 nm FWHM is structureless, as illustrated in Fig. 3. Among the different rare gas hosts, only in solid Ne is the XeF($D \rightarrow X$) emission vibrationally resolved.[21,22] The emission maximum in Ne matrices has been assigned to the $v' = 0 \rightarrow v'' = 2$ transition.[22] The assignment is in agreement with the gas phase analysis of the $D \rightarrow X$ emission, where the rotationless $D(v' = 0)$ state, the transition with the largest Franck–Condon factor is the one leading to $X(v'' = 2)$.[23] It may therefore be expected that in Kr as well, the $D \rightarrow X$ transition is peaked near $v'' = 2$ of the X state. The fluorescence lifetime of the D state is measured to be 9.8 (± 0.4) ns, independent of temperature, which would imply that the relaxation is dominated by radiation. Given the radiative lifetime τ and the spontaneous emission line shape $g(\nu)$, the stimulated emission cross section σ_s for the $D \rightarrow X$ transition can be obtained as

$$\sigma_s = (c^2/8\pi n^2 \nu^2 \tau) g(\nu) \qquad (1a)$$

at line center, the cross section can be well approximated as

$$\sigma_s(0) = (n/8\pi c\tau)(\lambda^4/\Delta\lambda) = 2\times 10^{-16}\ \text{cm}^2 \qquad (1b)$$

in which n is the index of refraction of solid Kr, ν is the emission frequency, c is the speed of light, τ is the radiative lifetime of XeF(D), and λ and $\Delta\lambda$ are the emission center and width, respectively. The cross section obtained in Eq. 1(a) is typical of diatomic exciplexes.[20] It is also possible to infer from the excitation profile of Fig. 2(b) that the $D \leftarrow X$ absorption cross section is an order of magnitude smaller, $\sim 2\times 10^{-17}$ cm^2 at the pump wavelength.

Upon excitation of the solid with increasingly higher pump powers, the on-axis emission is observed to collapse to a FWHM as narrow as 0.76 nm (see Fig. 3). Along with the spectral collapse, the main peak undergoes a 2 nm blue shift relative to the fluorescence maximum. The spectral collapse is accompanied by a superlinear increase in emission intensity along the pump axis. A typical example for the dependence of on-axis emission linewidth and intensity on pump fluence is shown in Fig. 4. The abscissa in the figure is based on the pump beam waist measured in vacuum—possibilities of self-focusing inside the crystal are not taken into account. It can be seen in Fig. 4 that the emission linewidth remains constant and its intensity increases linearly for pump fluences up to ~ 5 MW cm^{-2}. Above that limit, the linewidth begins to narrow and the emission intensity grows by three orders of magnitude for a sixfold increase in pump fluence. The spectral collapse, together with the exponential increase of the on-axis emission with pump intensity, are clear indications of amplified spontaneous emission.

The formulation of spectral narrowing due to amplified spontaneous emission is well known,[24] and has previously been applied to solid state exciplex lasers to extract gain parameters of the system.[1,2] Spontaneous emission with the spectral distribution of the fluorescence line shape $g(\nu)$ will emerge after traveling a distance r in the inverted medium as $g(\nu)e^{\alpha r}$ (α = net gain coefficient). Integration over r, over the full length l of the cylinder, yields the spectral distribution of the amplified spontaneous emission

$$I(\nu) = g(\nu)(e^{\alpha l} - 1)/\alpha. \qquad (2)$$

In the absence of losses, α is given as the product of the inverted population and the stimulated emission cross section $(N_2 - N_1)\sigma_s$. For $\alpha l \ll 1$, the spontaneous emission line shape is retrieved in Eq. (2); while for $\alpha l \gg 1$, the amplified emission line shape collapses due to the spectral dependence of σ_s given in Eq. (1). In the limit of large gain, the net gain-length product can be obtained from spectral widths as[23]

$$\alpha l = (\Gamma'/\Gamma)^2 \qquad (3)$$

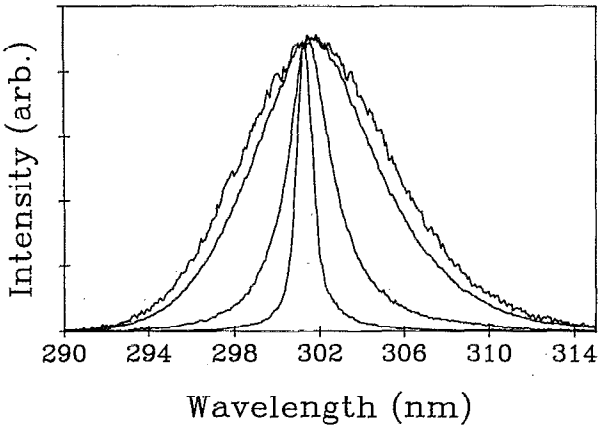

FIG. 3. Emission profile of the XeF $D \rightarrow X$ transition with different pump laser powers at 260 nm. Pump powers corresponding to emission from the broadest to the narrowest are 0.5, 13.5, 25, and 30 MW cm^{-2}. The spot size of the excitation laser is estimated to be 0.003 cm^2.

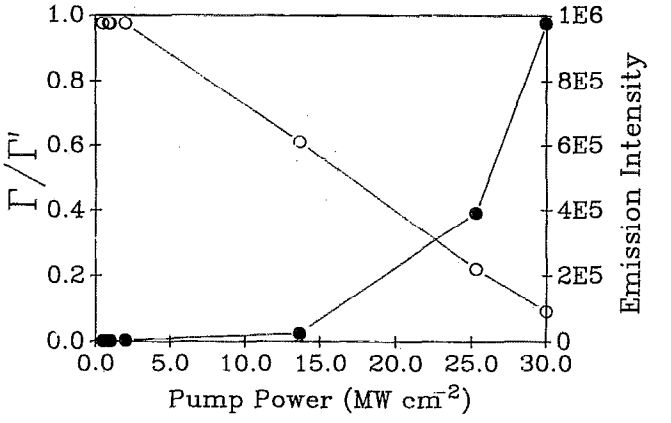

FIG. 4. Emission intensity (filled circles, right ordinate) and the linewidth ratio (open circles, left ordinate) of the XeF $D \rightarrow X$ transition as a function of pump power at 260 nm.

Downloaded 17 Feb 2004 to 128.200.47.19. Redistribution subject to AIP license or copyright, see http://jcp.aip.org/jcp/copyright.jsp

in which $\Gamma' =$ FWHM of fluorescence $= 8.2$ nm, $\Gamma =$ FWHM of amplified emission. At full spectral collapse, $\alpha l = 115$. In the present, $l = 1$ cm; therefore a net gain α in excess of 100 cm^{-1} is directly observed (in order to avoid multipassing by reflection at the crystal/vacuum interfaces, the measurements were conducted with the pump beam entering at a skew angle to the surface normal). The same limit was reached in several different crystals under similar conditions and at temperatures varying between 20 and 35 K. In all cases, attempts to further increase the observed gain by tighter focusing of the pump beam resulted in damage of the solid.

The observed gain is in accord with optimal parameters of the system. In the absence of losses, the gain coefficient should be given as $\alpha = (N_2 - N_1)\sigma_s(0)$; where N_2 and N_1 refer to the populations in $v' = 0$ of XeF(D) and to $v'' \sim 2$ of XeF(X), respectively. Given the cryogenic temperature of the system, the assumption $N_1 = 0$ is well justified. At the highest pump intensity, a photon density of $\sim 5 \times 10^{17}$ cm^{-3} is deposited in the sample (1 mJ, 0.6 mm beam waist). If we assume that N_2 is generated with unit quantum yield and use $\sigma_s(0)$ calculated in Eq. 1(b), a maximum gain coefficient of $\alpha_{max} = 100$ cm^{-1} would be expected. The good agreement of this determination with the gain measured from the spectral collapse is perhaps fortuitous. First, there are unavoidable scattering losses at both pump and emission wavelengths. Second, there are obvious loss mechanisms in the system. As an example, the observed emissions from the B, C, and triatomic exciplexes imply that the photogeneration quantum yield of XeF(D) is less than unity. Moreover, and although the extent is not known, nonradiative relaxation from the directly pumped states is expected to further reduce the pumping efficiency. Finally, the $D \rightarrow X$ emission overlaps the $B \leftarrow X$ absorption; and the blue shift of the collapsed line may be indicative of the significance of this absorption loss. For a homogeneously broadened fluorescence profile, due to the λ^3 dependence of the stimulated emission cross section, a red shift relative to the fluorescence maximum should be expected upon self-amplification. The observation of the blue shift implies a reabsorption profile that increases with wavelength. This is consistent with the $B \leftarrow X$ absorption which peaks near 345 nm.[21] In short, significant losses should contribute to the observed net gain, which is not reflected in the estimated gain coefficient based on the pump parameters. A reduction in the waist of the pump beam in the crystal would lead to a higher photon density and therefore to a larger value of α_{max}—one that could account for losses in the system.

Even in the presence of losses, the net gain coefficient is expected to be linearly proportional to the excited state number density and therefore to pump intensity I_p. Therefore, according to Eq. (3), a plot of Γ/Γ' vs $(I_p)^{-1/2}$ should yield a straight line passing through the origin. The plot of experimental data in this form in Fig. 5 shows that the spectral collapse begins in a superlinear fashion at low pump powers and only at high pump powers does it yield the expected linear behavior (inset to Fig. 5). Note that due to the abscissa used, the linear regime is deceptively compressed—the data in the inset corresponds to a fourfold increase in pump

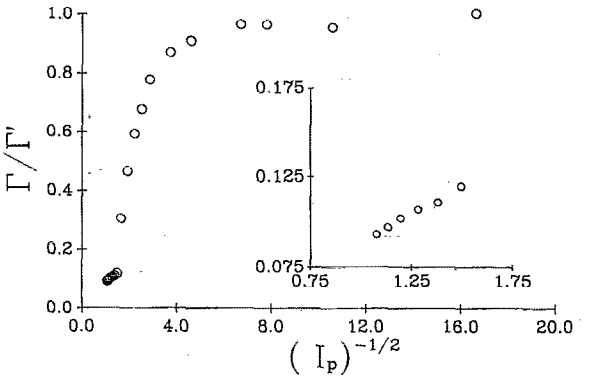

FIG. 5. Linewidth ratio Γ/Γ' as a function of the square root of the pump power $(I_p)^{-1/2}$. The initial spectral collapse begins at a superlinear rate at low pump powers. The insert shows the linear relationship which extrapolates to the origin for high pump powers.

intensity. We conclude that at intermediate pump powers, the excited state population density has a superlinear dependence on pump intensity. An electrostrictive mechanism, which leads to self-focusing of the beam with increasing pump powers, could explain this behavior. Further evidence to this effect is obtained from the observed divergence of the amplified beam.

At the high pump powers, the emerging ASE beam becomes clearly visible on a fluorescent screen. Using a 295 nm long-pass filter to eliminate residual pump photons, the beam energy was directly measured with a Joulemeter and a calibrated photodiode. For a pump energy of 1 mJ, 8 ($\pm$ 3) μJ is contained in the forward propagating ASE at 301 nm, from which a conversion quantum efficiency of $\phi = 1.4\%$ can be deduced. After inserting a limiting aperture, a divergence of 5($\pm$ 1) mrad was measured from the projection of the beam on a screen placed 85 cm from the aperture. The divergence of the amplified spontaneous emission is expected to be given by the aspect ratio of the gain volume. For a gain length of 1 cm, the measured divergence would imply a beam cross section of 50 μm—an order of magnitude less than the pump beam cross section in vacuum. Visual inspection of the side-light fluorescence gave no evidence for formation of filaments; however, self-focusing into a single filament could not be excluded as a possibility. We note that the visible emission is due to the lower charge transfer states, which although decoupled from the D state, would be expected to follow the spatial profile of the pump beam. In addition to rationalizing the observed small divergence of the amplified spontaneous emission beam, self-focusing would explain: (a) the observed optical damage of the crystal with small changes in focal waist of the pump beam; (b) the observed net gain without the exclusion of the expected losses; (c) the low conversion efficiency despite the large gain in the amplified beam; (d) and most significantly, the superlinear dependence of the excited state population density on pump intensity. The rather abrupt connection between the linear and nonlinear regimes shown in Fig. 5 can be ascribed to filament formation. The pumped volume cross section is expected to reach a minimum waist when self-focusing is counteracted by diffraction.[25] Above such a limit, the filament can be regarded as a linear waveguide.

Downloaded 17 Feb 2004 to 128.200.47.19. Redistribution subject to AIP license or copyright, see http://jcp.aip.org/jcp/copyright.jsp

Finally, we note that in the present experiments, there is no independent input as to the ground state XeF number density. Although in F_2 doped solid Ar (Ref. 5) and solid Kr (Ref. 16) it has previously been shown that the molecular photodissociation can be carried out to completion, in ternary solids at high concentrations a photochemical steady state is to be expected as discussed in the experimental section. If all F_2 in the sample ($\sim 10^{19}$ cm^{-3}) were photoconverted to XeF then given an absorption cross section of $\sim 10^{-17}$ cm^2, the pump beam would only penetrate a depth of $\sim 1\,\mu$m in the solid. In fact, the pump beam penetrates the entire 1 cm length of the solid and a residual pump intensity of $\sim 1\%$ is observed to be transmitted. This can be rationalized by one of two possible explanations: only 1% of the original F_2 is converted to XeF, or due to self-focusing the pump fluence is increased by two orders of magnitude. The latter is in good agreement with the tenfold reduction in pump waist deduced from the divergence measurements.

There are several electrostrictive mechanisms that may lead to self-focusing in solids.[25] A rather obvious consideration in the present case is the dramatic change of molecular dipoles that accompanies charge transfer transitions in rare gas halides. As a general rule, the ground states of rare gas halides are characterized by van der Waals potentials with little charge transfer character.[20] The optically accessed excited states in these systems are fully ionic, with molecular dipoles of ~ 10 D. At doping densities of 1:3000, exciplex number densities as high as 10^{19} cm^{-3} are possible in such solids. As a result, a very large, instantaneous jump in the dielectric constant of the medium is to be experienced in the pumped volume. Thus, if the spatial profile of the pump beam even remotely resembles a Gaussian, the leading edge should provide a waveguide for the trailing pulse. The effect observed in the present case should therefore be fairly general to all condensed phase optically pumped exciplex lasers. Furthermore, in crystalline solids, long dephasing times for the excited state dipoles are to be expected. It would then be interesting to investigate the effect of exciting such media with pump pulses of well-characterized mode structure and coherence lengths approaching the gain length of the medium. Under such conditions, it should be possible to create a phased array of dipoles in a high gain medium, and Dicke type superradiance,[26] and ultrashort laser action are two processes that should be observeable.[27]

VI. CONCLUSIONS

XeF in crystalline Kr provides another example of an efficient solid state exciplex laser. The large gain observed in the present case is comparable to those previously reported for XeF($B \rightarrow X$) and ($C \rightarrow A$) in crystalline Ar.[1] The conversion efficiency of 1% is an order of magnitude less in the present system, which indicates the presence of significant loss channels. Compelling evidence for self-focusing of the pump beam is obtained from the observations of superlinear dependence of the gain coefficient on pump intensity and from the small divergence of the amplified beam. This, in effect, would result in increased gain and reduced conversion efficiency, since the amplification occurs in a volume smaller than that of the pump volume measured in vacuum. The highly nonlinear nature of the medium is to be expected due to the large number densities of exciplexes and the large dipole associated with the covalent-to-ionic transitions.

These results are particularly significant, since the triatomic exciplex KrXeF is present in the system as the more stable charge transfer complex. Evidently, XeF(D) is isolated from the lower charge transfer manifold, which besides the triatomic includes XeF(B) and (C) states. This raises the possibility of observing gain on the KrF(D) state in solid Ar, even though the lower charge transfer manifold in that case is prevented from lasing due to reabsorptions.[4]

Although general principles guide the behavior of the solid state rare gas halides as laser media, the specific details of energy transfer and excited state reabsorption dynamics will be necessary for evaluation of individual members of this large family of X:Rg:Rg′ ternary solids. The prospects of developing deep ultraviolet lasers in such solids, in particular, in lighter rare gas–heavier halogen pairs remains a realistic goal. Several candidates for such applications have recently been characterized in matrices using synchrotron radiation sources.[28] Given the highly nonlinear characteristics of these gain media, it will be particularly interesting to observe the photodynamics of coherently prepared exciplexes.

ACKNOWLEDGMENTS

This research was supported through a grant from the National Science Foundation ECS-8914321 and a contract from the U.S. Air Force Astronautics Laboratory S04611-90-K-0035. A grant from the Academy of Finland to H. Kunttu during his stay at Irvine is gratefully acknowledged.

[1] N. Schwentner and V. A. Apkarian, Chem. Phys. Lett. **154**, 413 (1989).
[2] A. I. Katz, J. Feld, and V. A. Apkarian, Opt. Lett. **14**, 441 (1989).
[3] M. E. Fajardo, L. Wiedeman, and V. A. Apkarian, *Digest of International Quantum Electronics Conference* (Optical Society of America, Washington, D.C., 1987), paper PD-16; V. A. Apkarian, Proceedings of the International Conference on Lasers '89, p. 121.
[4] H. Kunttu, J. Feld, R. Alimi, A. Becker, and V. A. Apkarian, J. Chem. Phys. **92**, 4856 (1990).
[5] J. Feld, H. Kunttu, and V. A. Apkarian, J. Chem. Phys. **93**, 1009 (1990).
[6] N. Schwentner and V. A. Apkarian (unpublished data).
[7] M. E. Fajardo and V. A. Apkarian (unpublished data).
[8] F. Okada and V. A. Apkarian, J. Chem. Phys. **94**, 133 (1991).
[9] M. E. Fajardo and V. A. Apkarian, Chem. Phys. Lett. **134**, 51 (1987).
[10] L. Wiedeman, M. E. Fajardo, and V. A. Apkarian, Chem. Phys. Lett. **134**, 55 (1987).
[11] F. K. Tittel, M. Smayling, W. L. Wilson, and G. Marowsky, Appl. Phys. Lett. **37**, 862 (1980).
[12] F. K. Tittel, W. L. Wilson, R. E. Stickel, G. Marowsky, and W. E. Ernst, Appl. Phys. Lett. **36**, 405 (1980).
[13] D. B. Geohegan and J. G. Eden, J. Chem. Phys. **89**, 3410 (1988).
[14] H. Kunttu, E. Sekreta, and V. A. Apkarian (in preparation).
[15] W. Rudnick, R. Haensel, H. Nahme, and N. Schwentner, Phys. Status Solidi A **87**, 319 (1985).
[16] H. Kunttu, and V. A. Apkarian, Chem. Phys. Lett. **171**, 423 (1990).
[17] H. Helm, D. L. Huestis, M. J. Dyer, and D. C. Lorents, J. Chem. Phys. **79**, 3220 (1983); G. Black, R. L. Sharpless, D. C. Lorents, D. L. Huestis, R. A. Gutcheck, T. D. Bonifield, D. A. Helms, and G. K. Walters, *ibid.* **75**, 4840 (1981).
[18] E. Sekreta, P. Ashjian, and V. A. Apkarian (to be published).
[19] P. J. Hay and T. H. Dunning, Jr., J. Chem. Phys. **69**, 2209 (1978).
[20] *Topics in Applied Physics* edited by C. K. Rhodes (Springer, New York,

Downloaded 17 Feb 2004 to 128.200.47.19. Redistribution subject to AIP license or copyright, see http://jcp.aip.org/jcp/copyright.jsp

1984), Vol. 30.
[21] B. S. Ault and L. Andrews, J. Chem. Phys. **64**, 3075 (1976); **65**, 4192 (1976).
[22] J. Goodman and L. E. Brus, J. Chem. Phys. **65**, 3808 (1976).
[23] P. C. Tellinghuisen, J. T. Tellinghuisen, J. A. Coxon, J. E. Velazco, and D. W. Setser, J. Chem. Phys. **68**, 5187 (1978).
[24] A. Yariv, *Quantum Electronics*, 2nd ed. (Wiley, New York, 1975), Chap. 12.
[25] Y. R. Shen, *The Principles of Nonlinear Optics* (Wiley, New York, 1984), Chap. 17.
[26] R. H. Dicke, Phys. Rev. **93**, 99 (1954).
[27] See, e.g., E. D. Trifonov, in *Zero-Phonon Lines*, edited by O. Sild and K. Haller (Springer, New York, 1986), pp. 157–163.
[28] J. LeCalvè and P. Gürtler, J. Chim. Phys. **86**, 1849 (1989).

Downloaded 17 Feb 2004 to 128.200.47.19. Redistribution subject to AIP license or copyright, see http://jcp.aip.org/jcp/copyright.jsp